

# Loop unitary and phase band topological invariant in generic multi-band Chern insulators

Xi Wu\*

*School of Physics, Henan Normal University, Xixiang 453007, China*

Ze Yang and Fuxiang Li

*School of Physics and Electronics, Hunan University, Changsha 410082, China*

(Dated: July 1, 2024)

Quench dynamics of topological phases have been studied in the past few years and dynamical topological invariants are formulated in different ways. Yet most of these invariants are limited to minimal systems in which Hamiltonians are expanded by Gamma matrices. Here we generalize the dynamical 3 winding number in two-band systems into the one in generic multi-band Chern insulators and prove that its value is equal to the difference of Chern numbers between post-quench and pre-quench Hamiltonians. Moreover we obtain an expression of this dynamical 3 winding number represented by gapless fermions in phase bands depending only on the phase and its projectors, so it is generic for the quench of all multi-band Chern insulators. Besides, we obtain a multifold fermion in the phase band in  $(\mathbf{k}, t)$  space by quenching a three-band model, which cannot happen for two band models.

## I. INTRODUCTION

Topological phases, as new phases of matter, were originally proposed in static systems [1, 2]. In the past decade, more and more research have been investigated in dynamical systems such as Floquet systems[3–17] under a periodic driving Hamiltonian in which topological invariants are studied. Besides, explorations of topological phases after a quench are widely performed in the past years both in experiments[18–20] and in theory[21–25]. Based on the method of momentum resolved tomography, the information of time evolution of the wave functions is extracted and thus related with topology of the band insulators..

Although Chern number after quench[8, 26] is shown to be invariant under time evolution, different approaches have been taken to look for dynamical topological invariants. One approach is the so-called dynamical bulk-edge correspondence[27–35] to construct topological invariant by the time-averages of observables in the long-time limit, around the so-called band-inversion surfaces. This approach is successful not only in a sudden quench but also in a slow quench [36, 37]. There is another approach of constructing dynamical topological invariants which is based on a periodic time-momentum manifold by a rescaling of time. This approach also relates the dynamical topological invariants with static topological invariants. These includes the one for the one dimensional models [38] and Hopf invariant [39–41], loop unitary and its homotopy invariant[42, 43] for the quench process of Chern insulators/Hopf insulators in two/three dimensions.

Dynamical topological invariants proposed in various of dimensions above are mainly for minimal models of topological phases, in which Hamiltonians are expanded by Gamma matrices. The minimal models are the simplest models for Chern insulators. However, in more generic situations in condensed matter physics, multi-band Chern insulators beyond these are

encountered[44]. For a better understanding of the mathematics and the physics, the generalized Bloch spheres were introduced[45–49], which shows the complexity of the study of generic multi-band Chern insulators even in the static situation. Due to this complexity, an explicit picture for the quench dynamics of multi-band insulators and formulation of its dynamical topological invariants have been delayed comparing with the minimal models.

Recently, the time-evolving wave function of these Chern insulators from quench were successfully mapped out, using the description of nested-sphere [50]. So the quench dynamics for multi-band Chern insulators based on the coherence vector on the generalized Bloch sphere becomes manageable. It is therefore fully practical and important to construct a dynamical topological invariant for multi-band Chern insulators. Among the dynamical topological invariants mentioned above, the homotopy invariant of the loop unitary proposed in [42] is a promising candidate to describe the quench process of multi-band insulators because it is defined by the Wess-Zumino-Witten term which is not limited by the form of the Hamiltonian. In the two-band model this dynamical homotopy invariant, measuring the difference of post- and prequench Chern numbers, also manifests as defects in phase bands, which are Weyl fermions in the time-momentum manifold. This is a new picture that relates gapped and gapless fermions in different dimensions which is not originated from the traditional bulk-edge correspondence[51–53]. Note that this 3 winding number can be related to 4 dimensional Pontryagin class by a dimensional extension[54]. Two natural question arise if we generalize the loop unitary to multi-band insulators: Will the Wess-Zumino-Witten term give an integer valued homotopy invariant? Will this dynamical homotopy invariant also manifest itself as gapless fermions generically, and will there be multifold fermions as in the static case[55–61]?

In this work, we answer these two questions. We generalize the loop unitary of Chern insulators into multi-band models by a properly defined time-rescaling for each band. Based on this condition, we prove that the corresponding homotopy invariant is an integer and that its value is equal to the differ-

\* wuxi@htu.edu.cn

ence of post-quench and pre-quench Chern numbers. This is done in Sec. (II). Moreover we express this homotopy invariant by phase bands of the loop unitary, with an interpretation as defects of phase bands. This gives the generic correspondence between static gapped fermions and dynamical gapless fermions after quench. Using eigenprojectors instead of expansion by Pauli matrices, our results can describe quench process of models having any number of bands, but we also provide formulae for Hamiltonians expanded by  $\text{su}(N)$  algebras. This is done in Sec.(III). Finally, in Sec.(IV) we find an example that a three-fold fermion appears as the defect of phase band in a quench of a three band Chern insulator, showing its phase band dispersion and Berry curvature vector field. In Sec.(V) we discuss several topics as future directions.

## II. LOOP UNITARY FOR QUENCH DYNAMICS IN GENERIC MULTI-BAND CHERN INSULATORS

In this section, we briefly review the setup and results of [42] and then explain by an appropriate band-flattening these can work for a generic multi-band insulators. In the end of this section, we also explain that an inappropriate band-flattening may even lead to non-integer-valued 3-winding number. In [42] the loop unitary operator

$$U_l(t) = e^{-iht} e^{ih_0 t} \quad (1)$$

with its homotopy invariant, which is a 3-winding number/Wess-Zumino-Witten term

$$W_3[U_l] = \frac{1}{24\pi^2} \int_{T_3} d^2\mathbf{k} dt \epsilon^{\mu\nu\rho} \text{Tr}[(U_l^\dagger \partial_\mu U_l)(U_l^\dagger \partial_\nu U_l)(U_l^\dagger \partial_\rho U_l)] \quad (2)$$

were introduced to describe the quench dynamics for 2 band Chern insulators.  $h$  and  $h_0$  are the flattened post-quench and pre-quench Hamiltonians with band-flattening given by the replacement  $H \rightarrow h = H/E_{\mathbf{k}}$  and  $H_0 \rightarrow h_0 = H_0/E_{0\mathbf{k}}$ . Its value is equal to the difference of two static Chern numbers:

$$W_3[U_l] = \mathcal{C}_f - \mathcal{C}_i, \quad (3)$$

in which  $\mathcal{C}_{i/f}$  represent the Chern number of pre-quench and post-quench Hamiltonian. Unlike the static Chern numbers in which band-flattening only serves as a computation technique and does not change the topology, the loop unitary and its homotopy invariant includes band-flattening as part of the definition. This is required to ensure the periodicity in the time direction otherwise the expression in Eq.(2) does not give an integer number. This is the same situation in [39, 40]. The proof in their paper used Pauli matrices so it is limited to Clifford algebra. It was not clear from their paper whether their formalism is valid in the quench of generic multi-band Chern insulators, for instance for one with a Hamiltonian expanded by  $\text{su}(N)$  algebra. In the following, we show how the loop unitary is defined in such cases.

For multi-band Chern insulators, we apply the band-flattening given by

$$H \rightarrow \mathbf{h} = \sum_a \text{sgn}(E_a) P_a \quad \mathbf{h}_0 = \sum_a \text{sgn}(E_{0a}) P_{0a}, \quad (4)$$

in which  $E_a$  and  $E_{0a}$  are the energy eigenvalues,  $P_a$  and  $P_{0a}$  are the eigenprojectors and  $a$  labels the energy bands. Here the band-flattening is more restricted: all the energies below the Fermi surface should have the same value and the energies above the Fermi surface, too. Other less restricted choices may give integer number, but will not satisfy Eq.(3). And the loop unitary and its homotopy invariant take the same form as in Eq.(1) and Eq.(2) respectively. With Eq. (4) the multi-band loop unitary can be recast into

$$U_l(t) = (\cos t - i\mathbf{h} \sin t)(\cos t + i\mathbf{h}_0 \sin t). \quad (5)$$

One can check that  $U_l(t + \pi) = U_l(t)$  so the  $\pi$ -periodicity of time is ensured. For a generic  $N$ -band Hamiltonian, one can check that the band-flattening Eq. (4) makes  $U_l(t)$  an  $U(N)$  group element, but if the numbers of negative bands for post-quench and pre-quench Hamiltonian are the same then  $U_l(t)$  is a  $SU(N)$  group element. Both  $\pi_3[U(N)]$  and  $\pi_3[SU(N)]$  are integer valued. As time evolves, this  $W_3[U_l]$  counts the winding of the mapping from  $t, \mathbf{k}$  space to the generalized Bloch sphere for  $U(N)$  groups[45–49]. The value of  $W_3[U_l]$  is again equal to the difference of two static Chern numbers of bands below Fermi surfaces as in (3). If we connect the system with a chemical potential, we can change the Fermi surface. Then the band-flattening becomes

$$\begin{aligned} H' &= H - \mu \rightarrow \mathbf{h}' = \sum_a \text{sgn}(E_a - \mu) P_a \\ H'_0 &= H'_0 - \mu \rightarrow \mathbf{h}'_0 = \sum_a \text{sgn}(E_{0a} - \mu) P_{0a}. \end{aligned} \quad (6)$$

Since chemical potential term is proportional to identity matrix, the eigenfunctions are not changed at all. But the number of bands included in the static Chern numbers are changed. Therefore in multi-band Chern insulators, there is a way to measure static Chern number of each band through quench dynamics.

We give the complete prove of Eq.(3) for a generic multi-band case using a different method in Appendix(A) compared with [42], which is down-to-earth algebraic. The idea is very intuitive: first we show that  $W_3[U_l] = W_3[e^{iht}] + W_3[e^{ih_0 t}]$  where  $W_3[e^{-iht}]$  and  $W_3[e^{ih_0 t}]$  are obtained from replacing  $U_l$  by  $e^{-iht}$  and  $e^{ih_0 t}$  respectively (the result is mentioned in [13]). Second we show  $W_3[e^{-iht}] = \mathcal{C}_f$  and  $W_3[e^{ih_0 t}] = -\mathcal{C}_i$ . The first step is simple. Let us explain a little bit on the second step: With Eq.(4) we can write

$$U_1 = \sum_a e^{iE_a t} P_a(\mathbf{k}) = e^{iEt} P_+ + e^{-iEt} P_-, \quad (7)$$

where in  $P_+$  we include all the bands with energy above zero and  $P_-$  energy below zero and get

$$W_3[U_1] = -\frac{i}{2\pi} \int_{T_2} \sum_{E_a < 0} \text{Tr} P_a dP_a \wedge dP_a, \quad (8)$$

which is the sum of Chern numbers of negative energy bands. Similar mathematical proof was also used in showing the relation between Chern number and the 3-winding number in

Floquet systems [6, 62]. If we choose other types of band-flattening than Eq.(4), such that the energies differ from each other, we will get

$$W_3[U_1] = -\frac{1}{4\pi^2} \text{Tr} \sum_a \int_{T_3} d(iE_a t) \wedge P_a dP_a \wedge dP_a \quad (9)$$

instead. Such  $W_3[U_1]$  may not even be an integer because the periodicity may not be ensured and in general it is not proportional to the static Chern number. With the picture of gapless fermions given in the next section, we see that Eq.(3) relates two-dimensional gapped fermions with generic three-dimensional multifold gapless fermions.

### III. PHASE BAND CHERN NUMBER

In this section we show that the 3-winding number manifest as gapless fermions in the phase bands of the loop unitary. In phase-band formalism

$$U_l = \sum_a e^{i\phi_a(\mathbf{k}, t)} |\phi_a\rangle \langle \phi_a| = \sum_a e^{i\phi_a(\mathbf{k}, t)} P_a(\mathbf{k}, t). \quad (10)$$

Note that different from the eigenprojector in Eq.(4) here our eigenprojectors depend on time. In the remaining part of this section we write  $P_a$  for simplicity. One should beware the difference between usual energy bands and the phase bands: the gap-closing points are built-in structure of the periodic unitary

we have

$$\begin{aligned} W_3[U_l] &= \frac{1}{24\pi^2} \int_{T_3} \text{Tr} \left( U_l^\dagger dU_l \right)^3 \\ &= \frac{1}{24\pi^2} \int_{T_3} \text{Tr} \left( 3 \sum_a P_a d(i\phi_a) \sum_{b,c} e^{i(\phi_0 - \phi_c)} P_c dP_b \sum_{e,f} e^{i(\phi_e - \phi_f)} P_f dP_e \right. \\ &\quad \left. + \sum e^{i(\phi_a - \phi_b) + i(\phi_c - \phi_d) + i(\phi_e - \phi_f)} P_b dP_a \cdot P_d dP_c P_f dP_e \right). \end{aligned} \quad (14)$$

The first and the second term are calculated separately as

$$\begin{aligned} \text{1st term} &= 2 \sum_{a,b} d(i\phi_a) \wedge \text{Tr}(P_a dP_a \wedge dP_a) \\ &\quad - \sum_{a,b} d e^{-i(\phi_a - \phi_b)} \wedge \text{Tr}(P_a dP_a \wedge dP_b). \end{aligned} \quad (15)$$

$$\text{2nd term} = -3 \sum_{f,e} e^{-i(\phi_f - \phi_e)} d \text{Tr} (P_f \wedge dP_f \wedge dP_e) \quad (16)$$

Summing over the two terms we get

$$\begin{aligned} \textcircled{1} + \textcircled{2} &= 6 \text{Tr} \sum_a d(i\phi_a) \wedge P_a dP_a \wedge dP_a \\ &\quad - 3 \sum_{a,b} d(e^{-i(\phi_a - \phi_b)} \text{Tr}(P_a dP_a \wedge dP_b)) \end{aligned} \quad (17)$$

time-evolution at  $\sin(\phi_a) = 0$  and are thus not necessarily related with the topology. However, among all the gap-closing points there exist fermions that do count the topological number.

In Appendix(B) we showed that

$$W_3[U_l] = \frac{1}{4\pi^2} \text{Tr} \sum_a \int_{T_3} d(i\phi_a) \wedge P_a dP_a \wedge dP_a. \quad (11)$$

Eq.(11) is the key formula of our work. This is a sum of topological numbers of each phase band. The periodicity  $\phi_a$  is required by that of  $U_l$ . Since every  $\phi_a$  is periodic, the topological number of each phase band is an integer. Our proof is an algebraic proof, so Eq.(11) applies to any system with a Hermitian Hamiltonian. Therefore this result is valid and potentially useful for dynamical topological invariants even in integer quantum Hall effect.

The outline of the proof is as following: Starting from

$$W_3[U_l] = \frac{1}{24\pi^2} \int_{T_3} \text{Tr}[(U_l^{-1} dU_l)^3] \quad (12)$$

and using

$$\begin{aligned} U_l^{-1} dU_l &= \sum_a e^{-i\phi_a} P_a d \left( \sum_b e^{i\phi_a} P_b \right) \\ &= \sum_a P_a d(i\phi_a) + \sum_{a,b} e^{-i(\phi_a - \phi_b)} P_a dP_b \end{aligned} \quad (13)$$

and the second line vanishes after integration in  $T^3$ . Therefore we get Eq.(11).

Using the formula

$$\nabla \phi_a = \pi \text{sgn}(\cos \phi_a) \delta(\sin \phi_a) \nabla \sin \phi_a \quad (18)$$

from [63] we rewrite Eq.(11) as

$$W_3[U_l] = \frac{1}{4\pi} \sum_a \text{sgn}(\cos \phi_a) \int_{\mathbf{S}_p^a} d\mathbf{S}_p^a \cdot \boldsymbol{\Omega}^a \Big|_{\sin \phi_a = 0}, \quad (19)$$

where

$$\boldsymbol{\Omega}^a = i \text{Tr}(P_a \nabla P_a \times \nabla P_a) \quad (20)$$

is the Berry curvature of  $U_l$  and  $\mathbf{S}_p^a$  is in the direction of  $\nabla \sin \phi_a$ , surrounding the band-crossing points in the phase

band of  $\phi_a$ , and this gives opposite sign for phase bands with increasing  $\phi_a$  and decreasing  $\phi_a$  during time evolution. Eq.(19) gives another interpretation of  $W_3[U_l]$ , which is topological number of gapless fermions of phase bands. The way to evaluate this topological number is as following: We solve the eigenvector or the eigenprojector of  $U_l$ , calculate the Berry curvature and integrate it over  $(\mathbf{k}, t)$  space around the gapless points and then take a sum over all the points. The details will be given in Sec. (IV).

For an  $\text{su}(N)$  Hamiltonian expanded by generalized Gell-Mann matrices  $\lambda^m$  the coherence vector is defined as

$$S_a^m := \text{Tr}(\lambda^m P_a) \Leftrightarrow P_a =: \frac{\mathbb{1}}{N} + \frac{1}{2} S_a^m \lambda^m. \quad (21)$$

In such cases we can rewrite Eq.(19) as

$$W_3[U_l] = -\frac{1}{16\pi} \sum_a \text{sgn}(\cos \phi_a) \int_{\mathbb{S}_p^a} d\mathbf{S}_p^a \cdot f_{mnl} (S_a^m \nabla S_a^n \times \nabla S_a^l) \Big|_{\phi_a=\pi}, \quad (22)$$

where  $f_{mnl}$  is the anti-symmetric structure constant for  $\text{su}(N)$  algebra. (See Appendix(B) for derivation.) We see that besides the  $\pi$ -defect, the defect on  $\phi_a = 0$ , which we call 0-defect, may appear to represent the topological charge as well. It is easy to see that for 2-by-2 matrix this reduces to the formula for  $\pi$ -defect in [42].

#### IV. MULTIFOLD FERMIONS IN QUENCH DYNAMICS

The band-crossing points appearing in the quench dynamics of generic multi-band Chern insulators can take the form of not only Weyl fermions but also mutifold fermions[57], which cannot happen in two-band quench process. In this section, we show an example how a three-fold fermion appears in the phase band in the quench process.

Let us first explain the procedure of identifying a chiral gapless fermion which contributes to the dynamical winding number. Eq.(19) tells us that contributions come from the gapless points at  $\phi_a = 0$  or  $\phi_a = \pi$ , which means

$$\det(U_l \pm \mathbf{1}) = 0. \quad (23)$$

We choose appropriate  $(t, k_x, k_y) = (\bar{t}, \bar{k}_x, \bar{k}_y)$  to ensure this requirement, then expand  $U_l$  near  $(\bar{t}, \bar{k}_x, \bar{k}_y)$ . To get the value of dynamical winding number, we do the following

(1) Solve the eigen problem

$$U_l(\delta t, \delta k_x, \delta k_y) |\phi_a\rangle = e^{i\phi_a} |\phi_a\rangle;$$

(2) Calculate the Berry curvature  $\Omega_k^a = i\epsilon_{ijk} \partial_i \langle \tilde{\phi}_a | \partial_j | \tilde{\phi}_a \rangle$  where

$$|\tilde{\phi}_a\rangle = |\phi_a\rangle / \sqrt{\langle \phi_a | \phi_a \rangle}$$

Draw  $\Omega^a = (\Omega_1^a, \Omega_2^a, \Omega_3^a)$ .

We choose the pre-quench as

$$H_0 = \lambda_7, \quad (24)$$

and guided by intuition, the post-quench Hamiltonian as

$$H = h_x \lambda_2 + h_y \lambda_5 + h_z \lambda_7 \\ = \begin{bmatrix} 0 & -ih_x & -ih_y \\ ih_x & 0 & -ih_z \\ ih_y & ih_z & 0 \end{bmatrix} \quad (25)$$

with coefficients  $h_x = \sin k_x$ ,  $h_y = \sin k_y$ ,  $h_z = M - \cos k_x - \cos k_y$  and eigenvalues

$$E_i = \pm h, 0 = \pm \sqrt{\sum_{i=1}^3 h_i^2}, 0. \quad (26)$$

The post-quench Hamiltonian  $H$  looks similar as the two Qi-Wu-Zhang model but there are two key differences: First, there is a flat-band with zero Berry curvature between two other bands; second the Chern numbers of the two other bands are twice as that in Qi-Wu-Zhang model with same coefficients  $h_i$ . Strictly speaking, this is a conductor. (We can shift the total energy to make it an insulator, see Appendix (D)). By band-flattening we have

$$\mathbf{h} = (h_x \lambda_2 + h_y \lambda_5 + h_z \lambda_7)/h = \hat{h}_x \lambda_2 + \hat{h}_y \lambda_0 + \hat{h}_z \lambda_7 \quad (27) \\ \mathbf{h}_0 = \lambda_7$$

The loop unitary in this case is

$$U_l = e^{i\mathbf{h}t} e^{-i\mathbf{h}_0 t} \\ = (\cos t \mathbf{h}^2 + i \sin t \mathbf{h} + P_0) \cdot (\cos t \lambda_7^2 - i \sin t \lambda_7 + P_0^0), \quad (28)$$

in which  $P_0$  and  $P_0^0$  are the projection operators of the zero-energy bands of post- and pre-quench Hamiltonians respectively. A unique point of this example is that the zero energy band breaks the  $\pi$ -periodicity of time into  $2\pi$ -periodicity. From Fig.(1) we see there is a gapless point at  $t = \pi$ ,  $k_x = 0$ .

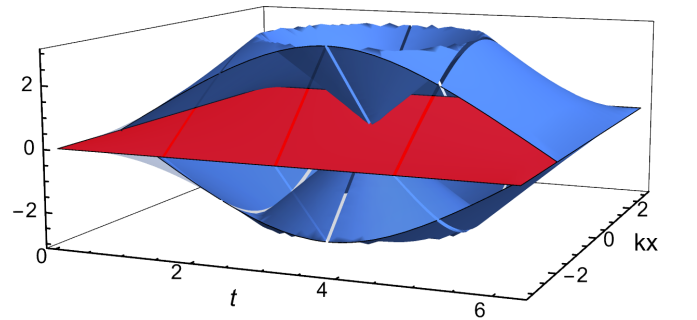


FIG. 1. Three phase band dispersions at  $k_y = 0$ , we made the bands transparent for the region  $-\pi < k_x < -\pi/2$ .

We call it a 0-defect because  $U_l(t = \pi, k_x = k_y = 0) = \mathbb{1}$

meaning the phase is 0 at this gapless point. We expand the loop unitary near this point:

$$\begin{aligned} U_l &= e^{ih(\delta t + \pi)} e^{-ih_0(\delta t + \pi)} \\ &\doteq \mathbb{1} - i \operatorname{sgn}(M - 2)(\delta k_x \lambda_5 - \delta k_y \lambda_2) \\ &\quad + i(\operatorname{sgn}(M - 2) - 1) \delta t \lambda_7. \end{aligned} \quad (29)$$

The detailed calculation is in Appendix(C). From the form it is easy to tell that this is a three-fold fermion mentioned in [57] carrying topological number 2.

From Eq.(22) we see that the coherence vector  $S_a^m$  have  $N^2 - 1$  components for each band for  $\mathfrak{su}(N)$ , so it is no longer practical to draw them as a vector field when  $N > 2$ . However, the Berry curvature always have three components. For the convenience of visualization, we draw the field of Berry curvature to represent the defects. Fig. (2) shows the Berry curvature of 0-defect we got from the example in this section.

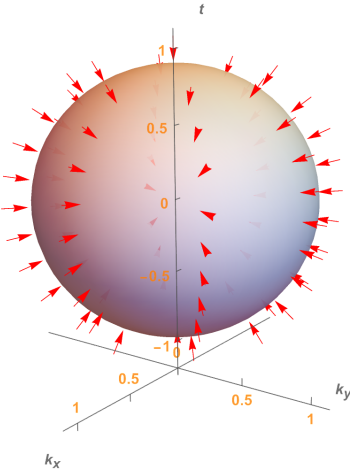


FIG. 2. Berry curvature vector of the lowest phase band of the 0-defect

## V. SUMMARY AND DISCUSSION

In this work, we studied the quench dynamics of multi-band Chern insulators in two-dimensions. We showed that for any number of bands, the difference of static Chern numbers of post-quench and pre-quench Hamiltonian can be represented by topological gapless fermions in the phase bands of the loop unitary operator. Moreover, we provide an example that a three-fold gapless fermions arises in the phase bands in a quench of a three band Chern insulator. We expect that gapless fermions with multi-fold degeneracy higher than three may appear if the Chern insulator has more bands. Further on this direction, one wonders whether other types of topological gapless structures such as nodal lines can appear in the phase bands and represent the static topology during quench dynamics. We leave this as a future exploration.

Both in the case of two-band models in[42] and our three-band models, we have checked that there is only one chiral

fermion in the whole period in the  $(\mathbf{k}, t)$  space. It is not surprising from the construction of our theory because the total chirality represents the difference of the static Chern numbers which must be nonzero in nontrivial quenches. This is also consistent with the results in [3, 10] that a single Weyl fermion exists in the quasienergy band of a Floquet unitary operator. The nature of phase band is different from energy band such that it does not satisfy the traditional Nielsen-Ninomiya theorem[64, 65].

[50] shows the protocol to mapped out all the coherence vectors through time-of-flight images in the generalized Bloch sphere for  $\mathfrak{su}(N)$  Hamiltonians. [66] gives a method to measure the defects directly for two band models, which can in principle be generalized. The combination of both methods may help detect defects in quench of multi-band models

As explained in [42], the Hopf invariant defined in [39, 40] works only for the case when the prequench Hamiltonian is topologically trivial and it suffers from the lack of gauge invariance. Suppose one accept these and define the Chern-Simons invariant for multi-band Hamiltonian quench processes, there is another challenge that gives limitation on the practical level: The Chern-Simons invariant becomes non-Abelian and the one dimensional linking number is replaced by at least a three dimensional one[67] where the dimension increases as the number of bands below Fermi surfaces grows so drawing the links becomes more and more complicated. However, the Berry curvature vector of the loop unitary are always three dimensional for the quench of two dimensional Chern insulators so it is rather convenient.

## ACKNOWLEDGEMENTS

This work was supported by the National Natural Science Foundation of China (Grants No. 11905054 and No. 12275075) and Doctoral scientific research foundation of Henan Normal University(Grants No. 5101029170913).

### Appendix A: The proof that $W_3 = C_f - C_i$

We start from

$$\begin{aligned} W_3[U_l] &= \frac{1}{24\pi^2} \int_{T_3} d^2\mathbf{k} dt \epsilon^{\mu\nu\rho} \\ &\quad \operatorname{Tr}[(U_l^{-1} \partial_\mu U_l)(U_l^{-1} \partial_\nu U_l)(U_l^{-1} \partial_\rho U_l)] \quad (\text{A1}) \\ &= \frac{1}{24\pi^2} \int_{T_3} \operatorname{Tr}[(U_l^{-1} dU_l)^3]. \quad (\text{A2}) \end{aligned}$$

We prove  $W_3 = C_f - C_i$  in two steps: First, since  $U_l = e^{-iht} e^{ih_0 t} = U_1 U_2$  where  $U_1 = e^{-iht}$ ,  $U_2 = e^{ih_0 t}$ , we show that

$$W_3[U_l] = W_3[U_1] + W_3[U_2] \quad (\text{A3})$$

where

$$\begin{aligned} W_3[U_a] &= \frac{1}{24\pi^2} \int_{T_3} d^2\mathbf{k} dt \epsilon^{\mu\nu\rho} \\ &\quad \operatorname{Tr}[(U_a^{-1} \partial_\mu U_a)(U_a^{-1} \partial_\nu U_a)(U_a^{-1} \partial_\rho U_a)], a = 1, 2. \end{aligned}$$

Second

$$W_3[U_1] = \mathcal{C}_f \quad (\text{A4})$$

$$W_3[U_2] = -\mathcal{C}_i. \quad (\text{A5})$$

Let's show Eq.(A3) in the following.

$$\begin{aligned} \text{Tr}[(U_l^{-1}dU_l)^3] &= \text{Tr}[(U_2^{-1}U_1^{-1}d(U_1U_2))^3] \\ &= \text{Tr}[(U_2^{-1}dU_2 + U_2^{-1}U_1^{-1}dU_1U_2)^3] \\ &= \text{Tr}[(U_2^{-1}dU_2)^3 + (U_1^{-1}dU_1)^3 + 3dU_2 \wedge U_2^{-1}dU_2 \wedge U_2^{-1}U_1^{-1}dU_1 + 3U_2^{-1}U_1^{-1}dU_1U_1^{-1}dU_1] \\ &= \text{Tr}[(U_2^{-1}dU_2)^3 + (U_1^{-1}dU_1)^3 - 3dU_2 \wedge dU_2^{-1} \wedge U_1^{-1}dU_1 - 3dU_1^{-1} \wedge dU_1 \wedge dU_2U_2^{-1}] \\ &= \text{Tr}[(U_2^{-1}dU_2)^3 + (U_1^{-1}dU_1)^3 - 3U_1^{-1}dU_1 \wedge d(U_2 \wedge dU_2^{-1}) + 3d(U_1^{-1} \wedge dU_1) \wedge U_2dU_2^{-1}] \\ &= \text{Tr}[(U_2^{-1}dU_2)^3 + (U_1^{-1}dU_1)^3 + 3d(U_1^{-1}dU_1 \wedge U_2dU_2^{-1})]. \end{aligned} \quad (\text{A6})$$

Since  $U_1$  and  $U_2$  are periodic in  $\mathbf{k}$  and  $t$ , the last term vanishes after integration and we get Eq.(A3). Moreover,

$$\text{Tr}(U_2^{-1}dU_2)^3 = -\text{Tr}(dU_2^{-1}U_2)^3 = -\text{Tr}(U_2dU_2^{-1})^3 \quad (\text{A7})$$

so Eq.(A3) can be rewritten as

$$W_3[U_l] = W_3[U_1] - W_3[U_2^{-1}]. \quad (\text{A8})$$

Next let's show Eq. (A4) and (A5), and this is an appetizer for a more general result in the next section. We start with

$$U_1 = \sum_a e^{-iE_a t} P_a(\mathbf{k}) = e^{-iEt} P_+ + e^{iEt} P_-, \quad (\text{A9})$$

where in  $P_+$  we include all the bands with energy above zero and  $P_-$  energy below zero and we assume band-flattening for all the bands(this assumption is removed in the proof in Appendix B). Then

$$\begin{aligned} W_3[U_1] &= \frac{1}{24\pi^2} \int_{T_3} \text{Tr}[(U_1^{-1}dU_1)^3] \\ &= \frac{1}{24\pi^2} \int_{T_3} \text{Tr}((e^{iEt} P_+ + e^{-iEt} P_-)d(e^{-iEt} P_+ + e^{iEt} P_-))^3 \\ &= \frac{1}{24\pi^2} \int_{T_3} \text{Tr} \left( -(P_+ - P_-)d(iEt) + ((e^{2iEt} - 1)P_+ - (e^{-2iEt} - 1)P_-)dP_- \right)^3 \\ &= \frac{-1}{8\pi^2} \int_{T_3} \text{Tr} \left[ (P_+ - P_-)d(iEt) \left( ((e^{2iEt} - 1)P_+ - (e^{-2iEt} - 1)P_-)dP_- \right)^2 \right] \end{aligned} \quad (\text{A10})$$

in the last step we used the fact that only the terms proportional to  $dt$  remains and  $P_-$  is independent of  $t$ . Then we expand Eq.(A10) using

$$\text{Tr}(P_+dP_+ \wedge P_+dP_+) = \text{Tr}(P_-dP_- \wedge P_-dP_-) = 0 \quad (\text{A11})$$

to get

$$\begin{aligned} W_3[U_1] &= \frac{-1}{4\pi^2} \int_{T_3} \text{Tr} \left[ d(iEt) \wedge ((1 - e^{2iEt})(e^{-2iEt} - 1))P_+dP_- \wedge P_-dP_- \right] \\ &= \frac{-1}{4\pi^2} \int_{T_3} d(iEt) \wedge ((2 - \cos(2Et))\text{Tr}P_-dP_- \wedge dP_-) \\ &= \frac{-1}{2\pi^2} \int_{T_3} d(iEt) \wedge \text{Tr}P_-dP_- \wedge dP_- \\ &= \frac{-i}{2\pi} \int_{T_2} \text{Tr}P_-dP_- \wedge dP_- \\ &= \frac{-i}{2\pi} \int_{T_2} \sum_{E_a < 0} \text{Tr}P_a dP_a \wedge dP_a. \end{aligned} \quad (\text{A12})$$

Therefore we see from Eq. (A12) that  $W_3[U_1]$  is indeed the static Chern number. And calculation for  $W_3[U_2]$  is the same so we get the conclusion of Eq.(A4) and (A5). Thus  $W_3 = \mathcal{C}_f - \mathcal{C}_i$  is proved.

### Appendix B: The proof of Eq.(11)

In this section, we solve  $W_3$  to get the phase band topological number. We again use Eq.(A2) and use  $U_l = \sum_a e^{i\phi_a(\mathbf{k},t)} P_a(\mathbf{k},t)$  where  $e^{i\phi_a(\mathbf{k},t)}$  are the phase bands and  $P_a(\mathbf{k},t)$  the corresponding projection operators, to expand it. We generalize the calculation of Eq.(A12) and prove the iden-

tity

$$W_3[U_l] = \frac{1}{4\pi^2} \int_{T_3} \text{Tr} \sum_a d(i\phi_a) \wedge P_a dP_a \wedge dP_a. \quad (\text{B1})$$

Note that

$$\begin{aligned} U_l^{-1} dU_l &= \sum_a e^{-i\phi_a} P_a d\left(\sum_b e^{i\phi_b} P_b\right) \\ &= \sum_a P_a d(i\phi_a) + \sum_{a,b} e^{-i(\phi_a - \phi_b)} P_a dP_b \end{aligned} \quad (\text{B2})$$

and the integrant in Eq. (A2) can be written as

$$\begin{aligned} &\text{Tr} \left( U_l^\dagger dU_l \right)^3 \\ &= \text{Tr} \left( \sum_a P_a d(i\phi_a) + \sum_{a,b} e^{i(\phi_a - \phi_b)} P_b dP_a \right)^3 \\ &= \text{Tr} \left( \left( \sum_a P_a d(i\phi_a) \right)^3 + 3 \left( \sum_a P_a d(i\phi_a) \right)^2 \sum_{c,d} e^{i(\phi_c - \phi_b)} P_d dP_c \right. \\ &\quad \left. + 3 \sum_a P_a d(i\phi_a) \left( \sum_{b,c} e^{i(\phi_b - \phi_c)} P_c dP_b \right)^2 + \left( \sum_{a,b} e^{i(\phi_a - \phi_b)} P_b dP_a \right)^3 \right) \quad (\text{B3}) \\ &= \text{Tr} \left( \underbrace{3 \sum_a P_a d(i\phi_a) \sum_{b,c} e^{i(\phi_b - \phi_c)} P_c dP_b \sum_{e,f} e^{i(\phi_e - \phi_f)} P_f dP_e}_{\textcircled{1}} \right. \\ &\quad \left. + \underbrace{\sum e^{i(\phi_a - \phi_b) + i(\phi_c - \phi_d) + i(\phi_e - \phi_f)} P_b dP_a \cdot P_d dP_c P_f dP_e}_{\textcircled{2}} \right) \end{aligned}$$

Using

$$\begin{aligned} P_b dP_a &= d(P_b \delta_{ab}) - dP_b P_a = dP_b (\delta_{ab} - P_a) \\ P_b dP_a P_d &= dP_b (\delta_{ab} P_d - \delta_{ad} P_d) = (\delta_{ab} - \delta_{ad}) dP_b P_d \end{aligned} \quad (\text{B4})$$

we calculate the two terms in the integrants separately.

$$\begin{aligned} \textcircled{1} &= \text{Tr} \left( \sum_a P_a d(i\phi_a) \sum_{b,c} e^{i(\phi_b - \phi_c)} P_c dP_b \sum_{e,f} e^{i(\phi_e - \phi_f)} P_f dP_e \right) \\ &= \text{Tr} \sum d(i\phi_a) e^{i(\phi_b - \phi_a)} P_a dP_b e^{i(\phi_e - \phi_f)} P_f dP_e \\ &= \text{Tr} \sum d(i\phi_a) e^{i(\phi_b - \phi_a) + i(\phi_e - \phi_f)} P_a dP_b P_f dP_e \\ &= \text{Tr} \sum d(i\phi_a) e^{i(\phi_b - \phi_a) + i(\phi_e - \phi_f)} (\delta_{ab} - \delta_{bf}) dP_a P_f dP_e \\ &= \text{Tr} \sum \left( d(i\phi_b) e^{i(\phi_e - \phi_f)} dP_b P_f dP_e + d(i\phi_a) e^{i(\phi_e - \phi_a)} dP_a P_f dP_e \right) \\ &= - \text{Tr} \sum d(i\phi_b) e^{i(\phi_e - \phi_f)} P_f dP_e dP_b \end{aligned} \quad (\text{B5})$$

In order to proceed, we use

$$\begin{aligned}
& \text{Tr}(P_a dP_b \wedge dP_c) \\
&= \langle \phi_a | d(|\phi_b\rangle\langle\phi_b|) \wedge d(|\phi_c\rangle\langle\phi_c|) | a \rangle \\
&= \langle \phi_a | d|\phi_b\rangle\langle\phi_b| \wedge d|\phi_c\rangle\delta_{ca} + \langle \phi_a | d|\phi_b\rangle d\langle\phi_c| | a \rangle \delta_{bc} \\
&\quad + \delta_{ab} \delta_{ca} d\langle\phi_b| d|c\rangle + \delta_{ab} d\langle\phi_b| |\phi_c\rangle d\langle\phi_c| | \phi_a \rangle \\
&= \delta_{ca} \text{Tr}(P_a dP_a \wedge dP_b) + \delta_{bc} \text{Tr}(P_a dP_b \wedge dP_b) \\
&\quad + \delta_{ab} \delta_{ca} \text{Tr}(P_a dP_a \wedge dP_a) + \delta_{ab} \text{Tr}(P_a dP_a \wedge dP_c).
\end{aligned} \tag{B6}$$

$$\begin{aligned}
&= \delta_{ca} \text{Tr}(P_a dP_a \wedge dP_b) + \delta_{bc} \text{Tr}(P_a dP_b \wedge dP_b) \\
&\quad + \delta_{ab} \delta_{ca} \text{Tr}(P_a dP_a \wedge dP_a) + \delta_{ab} \text{Tr}(P_a dP_a \wedge dP_c).
\end{aligned} \tag{B7}$$

Then the first term becomes

$$\begin{aligned}
\textcircled{1} &= 2 \sum_{a,b} d(i\phi_a) \wedge \text{Tr}(P_a dP_a \wedge dP_a) \\
&\quad - \sum_{a,b} d e^{-i(\phi_a - \phi_b)} \wedge \text{Tr}(P_a dP_a \wedge dP_b).
\end{aligned} \tag{B8}$$

Next let us calculate the second term. Using

$$\begin{aligned}
& \text{Tr}(P_b dP_a P_d dP_c P_f dP_e) \\
&= \text{Tr}((\delta_{ab} - \delta_{ad}) dP_b P_d dP_c P_f dP_e) \\
&= \text{Tr}((\delta_{ab} - \delta_{ad})(\delta_{cd} - \delta_{cf}) dP_b dP_d P_f dP_e)
\end{aligned} \tag{B9}$$

and

$$\begin{aligned}
& \sum_{a,b,c,d,e,f} e^{i(\phi_a - \phi_b) + i(\phi_c - \phi_d) + i(\phi_e - \phi_f)} (\delta_{ab} - \delta_{ad})(\delta_{cd} - \delta_{cf}) \\
&= \sum \left( e^{i(\phi_c - \phi_d) + i(\phi_e - \phi_f)} - e^{i(\phi_c - \phi_b) + i(\phi_e - \phi_f)} \right) (\delta_{cd} - \delta_{cf}) \\
&= \sum \left( e^{i(\phi_e - \phi_f)} - e^{i(\phi_d - \phi_b) + i(\phi_e - \phi_f)} - e^{i(\phi_e - \phi_d)} + e^{i(\phi_e - \phi_b)} \right)
\end{aligned} \tag{B10}$$

the second term becomes

$$\begin{aligned}
\textcircled{2} &= \sum \left( e^{i(\phi_e - \phi_f)} - e^{i(\phi_d - \phi_b) + i(\phi_e - \phi_f)} - e^{i(\phi_e - \phi_d)} \right. \\
&\quad \left. + e^{i(\phi_e - \phi_b)} \right) \text{Tr} dP_b dP_d P_f dP_e.
\end{aligned} \tag{B11}$$

Now for the four exponential terms, only the second one survives after integration:

$$\textcircled{2} = - \sum_{f,e,b,d} e^{-i(\phi_f - \phi_e) - i(\phi_b - \phi_d)} \text{Tr}(P_f dP_e dP_b dP_d) \tag{B12}$$

because

$$\begin{aligned}
& \sum_{b,d,e,f} \text{Tr} \left( e^{i(\phi_e - \phi_f)} dP_b dP_d P_f dP_e \right) \\
&= \sum \text{Tr} \left( e^{i(\phi_e - \phi_f)} dP_b (\delta_{df} dP_f - P_d dP_f) dP_e \right) \\
&= \sum \text{Tr} \left( e^{i(\phi_e - \phi_f)} (dP_b dP_f dP_e - dP_b P_d dP_f dP_e) \right) \\
&= 0 \\
& \int_{T^3} \sum \text{Tr} e^{i(\phi_e - \phi_d)} dP_b dP_d P_f dP_e \\
&= \int_{T^3} e^{i(\phi_e - \phi_d)} dP_b dP_d dP_e \\
&= \sum \text{Tr} \int_{T^3} \left( d \left( e^{i(\phi_e - \phi_d)} P_b dP_d dP_e \right) - d e^{i(\phi_e - \phi_d)} P_b dP_d dP_e \right) \\
&= \sum \text{Tr} \int_{\partial T^3} \left( e^{i(\phi_e - \phi_d)} P_b dP_d dP_e \right) \\
&= 0
\end{aligned} \tag{B13}$$



and with the same logic we have

$$\int_{T^3} \sum \text{Tr} e^{i(\phi_e - \phi_d)} dP_b dP_d P_f dP_e = 0.$$

Substituting into Eq.(B12) the following expression, which can be checked

$$\begin{aligned} & \text{Tr} (P_f dP_e dP_b dP_d) \\ &= \langle \phi_f | d | \phi_e \rangle d \langle \phi_e | d | \phi_f \rangle \delta_{eb} \delta_{fd} + \langle \phi_f | d | \phi_b \rangle d \langle \phi_b | \cdot | \phi_f \rangle \delta_{fe} \delta_{bd} \\ &+ d (\langle \phi_f | d | \phi_b \rangle \langle \phi_b | d | \phi_f \rangle) \delta_{fe} \delta_{df} + \langle \phi_f | d | \phi_e \rangle \langle \phi_e | d | \phi_b \rangle \langle \phi_b | d | \phi_f \rangle \delta_{fd} \\ &+ \langle \phi_f | d | \phi_e \rangle \langle \phi_e | d | \phi_b \rangle d \langle \phi_b | \cdot | \phi_f \rangle \delta_{bd} + \langle \phi_f | d | \phi_e \rangle d \langle \phi_e | \cdot | \phi_d \rangle d \langle \phi_d | \cdot | \phi_f \rangle \delta_{eb} \\ &+ d \langle \phi_b | \cdot | \phi_d \rangle d \langle \phi_d | \cdot | \phi_f \rangle d \langle \phi_f | \cdot | \phi_b \rangle \delta_{fe} \end{aligned}$$

we get

$$\textcircled{2} = -3 \sum_{f,e} e^{-i(\phi_f - \phi_e)} d \text{Tr} (P_f dP_f dP_e). \quad (\text{B14})$$

Summing over the two terms we get

$$\begin{aligned} \textcircled{1} + \textcircled{2} &= 6 \text{Tr} \sum_a d(i\phi_a) \wedge P_a dP_a \wedge dP_a \\ &- 3 \sum_{a,b} d(e^{-i(\phi_a - \phi_b)} \text{Tr}(P_a dP_a \wedge dP_b)) \quad (\text{B15}) \end{aligned}$$

and the second line vanishes after integration in  $T^3$ . Therefore we get Eq.(B1).

Now we use the projection operator formula for  $\text{su}(N)$  algebra

$$P_a = \frac{1}{N} + \frac{1}{2} \vec{S}_a \cdot \vec{\lambda}, \quad f_{mnl} = -\frac{i}{4} \text{Tr}(\lambda_m [\lambda_n, \lambda_l]) \quad (\text{B16})$$

to rewrite Eq.(20) as

$$\begin{aligned} \Omega_i^a &= i\epsilon_{ijk} \text{Tr} (P_a \partial_j P_a \partial_k P_a) \\ &= \frac{i}{8} \epsilon_{ijk} \text{Tr} (\lambda_m \lambda_n \lambda_l) S_a^m \partial_j S_a^n \partial_k S_a^l \\ &= \frac{i}{16} \epsilon_{ijk} \text{Tr} (\lambda_m [\lambda_n, \lambda_l]) S_a^m \partial_j S_a^n \partial_k S_a^l \\ &= -\frac{1}{4} f_{mnl} S_a^m (\nabla S_a^n \times \nabla S_a^l)_i \quad (\text{B17}) \end{aligned}$$

and therefore Eq.(22) is obtained.

### Appendix C: Expansion of $U_l$

In this section, we explain the expansion of  $U_l$  in Eq.(29) With the condition  $h_x = \sin k_x$ ,  $h_y = \sin k_y$ ,  $h_z = M -$

$\cos k_x - \cos k_y$ .

$$\begin{aligned} & U_l (\delta t, \delta k_x, \delta k_y) \Big|_{(t, k_x, k_y) = (\pi, 0, 0)} \\ &= (\cos t \mathbf{h}^2 + i \sin t \mathbf{h} + P_0) \\ &\quad \cdot (\cos t \lambda_7^2 - i \sin t \lambda_7 + P_0^0) \Big|_{(t, k_x, k_y) = (\pi, 0, 0)} \\ &= \left( -(\lambda_7^2 + \delta \mathbf{h}^2) + P_0^0 + i(-\delta t) \hat{h}_z \lambda_7 \right) \\ &\quad \cdot (-\lambda_7^2 + P_0^0 + i \delta t \lambda_7) \\ &= \mathbb{1} - i \delta t (1 - \hat{h}_z \Big|_{(0,0)}) - \delta \mathbf{h}^2 \Big|_{(0,0)} (-\lambda_7^2 + P_0^0) \quad (\text{C1}) \end{aligned}$$

$\delta \mathbf{h}^2 \Big|_{(0,0)}$  is calculated as following:

$$\begin{aligned} \mathbf{h}^2 &= \begin{pmatrix} \hat{h}_x^2 + \hat{h}_y^2 & \hat{h}_y \hat{h}_z & -\hat{h}_x \hat{h}_z \\ \hat{h}_y \hat{h}_z & \hat{h}_x^2 + \hat{h}_z^2 & \hat{h}_x \hat{h}_y \\ -\hat{h}_x \hat{h}_z & \hat{h}_x \hat{h}_y & \hat{h}_y^2 + \hat{h}_z^2 \end{pmatrix} \quad (\text{C2}) \\ \delta \mathbf{h}^2 \Big|_{(0,0)} &\doteq \begin{pmatrix} \delta k_x^2 + \delta k_y^2 & \hat{h}_z \delta k_y & -\hat{h}_z \delta k_x \\ \hat{h}_z \delta k_y & \delta k_x^2 & \delta k_x \delta k_y \\ -\hat{h}_z \delta k_x & \delta k_x \delta k_y & \delta k_y \end{pmatrix} \\ &\doteq \hat{h}_z \begin{pmatrix} 0 & \delta k_y & -\delta k_x \\ \delta k_y & 0 & 0 \\ -\delta k_x & 0 & 0 \end{pmatrix} \quad (\text{C3}) \end{aligned}$$

Then finally we get

$$\begin{aligned} & U_l (\delta t, \delta k_x, \delta k_y) \Big|_{(\pi, 0, 0)} \\ &= \mathbb{1} + i \delta t \lambda_7 \left( \hat{h}_z \Big|_{(0,0)} - 1 \right) \\ &\quad - \begin{pmatrix} 0 & \hat{h}_z \delta k_y & -\hat{h}_z \delta k_x \\ \hat{h}_z \delta k_y & 0 & 0 \\ -\hat{h}_z \delta k_x & 0 & 0 \end{pmatrix} \begin{pmatrix} 1 & & \\ & -1 & \\ & & -1 \end{pmatrix} \\ &= \mathbb{1} + i \delta t \lambda_7 \left( \hat{h}_z \Big|_{(0,0)} - 1 \right) + i \hat{h}_z \Big|_{(0,0)} (\lambda_2 \delta k_y - \lambda_5 \delta k_x) \\ &= \mathbb{1} - i \text{sgn}(M-2) (\delta k_x \lambda_5 - \delta k_y \lambda_2) + i (\text{sgn}(M-2) - 1) \delta t \lambda_7 \quad (\text{C4}) \end{aligned}$$

### Appendix D: Phase bands with energy shift

In Sec.(IV) we showed the three-fold fermion in the phase band with a  $2\pi$  period in time. We can add a chemical potential to shift the overall energy via Eq.(6). Then the two models become insulators and the period of time in loop unitary is changed back into  $\pi$ . The loop unitary in such case is

$$\begin{aligned} U_l &= e^{i(\mathbf{h}+P_0)t} e^{-i(\mathbf{h}_0+P_0^0)t} \\ &= (\cos t \mathbf{h}^2 + i \sin t (\mathbf{h} + P_0)) \cdot (\cos t \lambda_7^2 - i \sin t (\lambda_7 + P_0^0)) . \end{aligned}$$

However the sacrifice is that the defect is no longer three-fold. We show the plot of phase bands here.

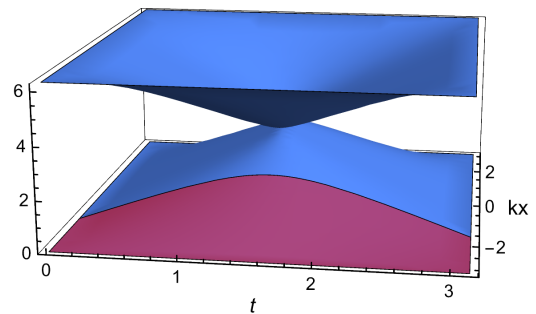


**(FIG. 3.)** Three phase band dispersions at  $k_y = 0$ , we made the second band transparent for the region  $-\pi < k_x < -\pi/2$ .

- 
- [1] M. Z. Hasan and C. L. Kane, *Rev. Mod. Phys.* **82**, 3045 (2010).
- [2] X.-G. Wen, *Quantum Field Theory of Many-Body Systems: From the Origin of Sound to an Origin of Light and Electrons* (Oxford Univ. Press, 2004).
- [3] T. Kitagawa, E. Berg, M. Rudner, and E. Demler, *Phys. Rev. B* **82**, 235114 (2010).
- [4] N. H. Lindner, G. Refael, and V. Galitski, *Nature Physics* **7**, 490 (2011).
- [5] L. Jiang, T. Kitagawa, J. Alicea, A. R. Akhmerov, D. Pekker, G. Refael, J. I. Cirac, E. Demler, M. D. Lukin, and P. Zoller, *Phys. Rev. Lett.* **106**, 220402 (2011).
- [6] M. S. Rudner, N. H. Lindner, E. Berg, and M. Levin, *Phys. Rev. X* **3**, 031005 (2013).
- [7] A. Gómez-León and G. Platero, *Phys. Rev. Lett.* **110**, 200403 (2013).
- [8] L. D'Alessio and M. Rigol, *Nature Communications* **6**, 8336 (2015).
- [9] A. C. Potter, T. Morimoto, and A. Vishwanath, *Phys. Rev. X* **6**, 041001 (2016).
- [10] S. Higashikawa, M. Nakagawa, and M. Ueda, *Phys. Rev. Lett.* **123**, 066403 (2019).
- [11] H. Hu, B. Huang, E. Zhao, and W. V. Liu, *Phys. Rev. Lett.* **124**, 057001 (2020).
- [12] R. Roy and F. Harper, *Phys. Rev. B* **96**, 155118 (2017).
- [13] S. Yao, Z. Yan, and Z. Wang, *Phys. Rev. B* **96**, 195303 (2017).
- [14] K. Yang, L. Zhou, W. Ma, X. Kong, P. Wang, X. Qin, X. Rong, Y. Wang, F. Shi, J. Gong, and J. Du, *Phys. Rev. B* **100**, 085308 (2019).
- [15] T. Li and H. Hu, *Nature Communications* **14**, 6418 (2023).
- [16] M. Jangjan and M. V. Hosseini, *Scientific Reports* **10**, 14256 (2020).
- [17] M. Jangjan, L. E. F. Foa Torres, and M. V. Hosseini, *Phys. Rev. B* **106**, 224306 (2022).
- [18] N. Fläschner, B. S. Rem, M. Tarnowski, D. Vogel, D.-S. Lühmann, K. Sengstock, and C. Weitenberg, *Science* **352**, 1091 (2016), <https://www.science.org/doi/pdf/10.1126/science.aad4568>.
- [19] E. Alba, X. Fernandez-Gonzalvo, J. Mur-Petit, J. K. Pachos, and J. J. Garcia-Ripoll, *Phys. Rev. Lett.* **107**, 235301 (2011).
- [20] P. Hauke, M. Lewenstein, and A. Eckardt, *Phys. Rev. Lett.* **113**, 045303 (2014).
- [21] M. D. Caio, N. R. Cooper, and M. J. Bhaseen, *Phys. Rev. Lett.* **115**, 236403 (2015).
- [22] M. D. Caio, N. R. Cooper, and M. J. Bhaseen, *Phys. Rev. B* **94**, 155104 (2016).
- [23] Y. Hu, P. Zoller, and J. C. Budich, *Phys. Rev. Lett.* **117**, 126803 (2016).
- [24] M. Tarnowski, F. N. Ünal, N. Fläschner, B. S. Rem, A. Eckardt, K. Sengstock, and C. Weitenberg, *Nature Communications* **10**, 1728 (2019).
- [25] F. N. Ünal, A. Bouhon, and R.-J. Slager, *Phys. Rev. Lett.* **125**, 053601 (2020).
- [26] L. Ulčakar, J. Mravlje, A. Ramšak, and T. c. v. Rejec, *Phys. Rev. B* **97**, 195127 (2018).
- [27] L. Zhang, L. Zhang, S. Niu, and X.-J. Liu, *Sci. Bull.* **63**, 1385 (2018).
- [28] L. Zhang, L. Zhang, and X.-J. Liu, *Phys. Rev. A* **99**, 053606 (2019).
- [29] Y. Wang, W. Ji, Z. Chai, Y. Guo, M. Wang, X. Ye, P. Yu, L. Zhang, X. Qin, P. Wang, F. Shi, X. Rong, D. Lu, X.-J. Liu, and J. Du, *Phys. Rev. A* **100**, 052328 (2019).
- [30] X.-L. Yu, W. Ji, L. Zhang, Y. Wang, J. Wu, and X.-J. Liu, *PRX Quantum* **2**, 020320 (2021).
- [31] L. Zhang, L. Zhang, and X.-J. Liu, *Phys. Rev. Lett.* **125**, 183001 (2020).
- [32] W. Sun, C.-R. Yi, B.-Z. Wang, W.-W. Zhang, B. C. Sanders, X.-T. Xu, Z.-Y. Wang, J. Schmiedmayer, Y. Deng, X.-J. Liu, S. Chen, and J.-W. Pan, *Phys. Rev. Lett.* **121**, 250403 (2018).
- [33] L. Li, W. Zhu, and J. Gong, *Science Bulletin* **66**, 1502 (2021).
- [34] X. Wu, P. Fang, and F. Li, *Phys. Rev. A* **107**, 052209 (2023).
- [35] B. Zhu, Y. Ke, H. Zhong, and C. Lee, *Phys. Rev. Res.* **2**, 023043 (2020).
- [36] J. Ye and F. Li, *Phys. Rev. A* **102**, 042209 (2020).
- [37] P. Fang, Y.-X. Wang, and F. Li, *Phys. Rev. A* **106**, 022219 (2022).
- [38] C. Yang, L. Li, and S. Chen, *Phys. Rev. B* **97**, 060304 (2018).
- [39] C. Wang, P. Zhang, X. Chen, J. Yu, and H. Zhai, *Phys. Rev. Lett.* **118**, 185701 (2017).
- [40] X. Chen, C. Wang, and J. Yu, *Phys. Rev. A* **101**, 032104 (2020).
- [41] N. Fläschner, D. Vogel, M. Tarnowski, B. S. Rem, D. S. Lühmann, M. Heyl, J. C. Budich, L. Mathey, K. Sengstock, and C. Weitenberg, *Nat. Phys.* **14**, 265 (2018).
- [42] H. Hu and E. Zhao, *Phys. Rev. Lett.* **124**, 160402 (2020).
- [43] H. Hu, C. Yang, and E. Zhao, *Phys. Rev. B* **101**, 155131 (2020).

- [44] R. Barnett, G. R. Boyd, and V. Galitski, *Phys. Rev. Lett.* **109**, 235308 (2012).
- [45] L. Jakóbczyk and M. Siennicki, *Physics Letters A* **286**, 383 (2001).
- [46] K. Zyczkowski and H.-J. Sommers, *Journal of Physics A: Mathematical and General* **36**, 10115 (2003).
- [47] G. Kimura, *Physics Letters A* **314**, 339 (2003).
- [48] M. S. Byrd and N. Khaneja, *Phys. Rev. A* **68**, 062322 (2003).
- [49] A. Graf and F. Piéchon, *Phys. Rev. B* **104**, 085114 (2021).
- [50] C. J. D. Kemp, N. R. Cooper, and F. N. Únal, *Phys. Rev. Res.* **4**, 023120 (2022).
- [51] Y. Hatsugai, *Phys. Rev. Lett.* **71**, 3697 (1993).
- [52] T. Fukui, *Phys. Rev. Res.* **2**, 043136 (2020).
- [53] K. Hashimoto, X. Wu, and T. Kimura, *Phys. Rev. B* **95**, 165443 (2017).
- [54] Z. Davoyan, W. J. Jankowski, A. Bouhon, and R.-J. Slager, *Phys. Rev. B* **109**, 165125 (2024).
- [55] J. L. Mañes, *Phys. Rev. B* **85**, 155118 (2012).
- [56] L. Liang and Y. Yu, *Phys. Rev. B* **93**, 045113 (2016).
- [57] B. Bradlyn, J. Cano, Z. Wang, M. G. Vergniory, C. Felser, R. J. Cava, and B. A. Bernevig, *Science* **353**, aaf5037 (2016), <https://www.science.org/doi/pdf/10.1126/science.aaf5037>.
- [58] P. Tang, Q. Zhou, and S.-C. Zhang, *Phys. Rev. Lett.* **119**, 206402 (2017).
- [59] G. Chang, S.-Y. Xu, B. J. Wieder, D. S. Sanchez, S.-M. Huang, I. Belopolski, T.-R. Chang, S. Zhang, A. Bansil, H. Lin, and M. Z. Hasan, *Phys. Rev. Lett.* **119**, 206401 (2017).
- [60] N. B. M. Schröter, D. Pei, M. G. Vergniory, Y. Sun, K. Manna, F. de Juan, J. A. Krieger, V. Süss, M. Schmidt, P. Dudin, B. Bradlyn, T. K. Kim, T. Schmitt, C. Cacho, C. Felser, V. N. Strocov, and Y. Chen, *Nature Physics* **15**, 759 (2019).
- [61] I. Robredo, N. Schröeter, C. Felser, J. Cano, B. Bradlyn, and M. G. Vergniory, (2024), 2404.17539.
- [62] P. Titum, E. Berg, M. S. Rudner, G. Refael, and N. H. Lindner, *Phys. Rev. X* **6**, 021013 (2016).
- [63] T. Bessho and M. Sato, *Phys. Rev. Lett.* **127**, 196404 (2021).
- [64] H. Nielsen and M. Ninomiya, *Nuclear Physics B* **185**, 20 (1981).
- [65] H. Nielsen and M. Ninomiya, *Nuclear Physics B* **193**, 173 (1981).
- [66] F. N. Únal, B. Seradjeh, and A. Eckardt, *Phys. Rev. Lett.* **122**, 253601 (2019).
- [67] T. Si, *Journal of Mathematical Physics* **46**, 122301 (2005), [https://pubs.aip.org/aip/jmp/article-pdf/doi/10.1063/1.2137721/15867792/122301\\_1\\_online.pdf](https://pubs.aip.org/aip/jmp/article-pdf/doi/10.1063/1.2137721/15867792/122301_1_online.pdf).